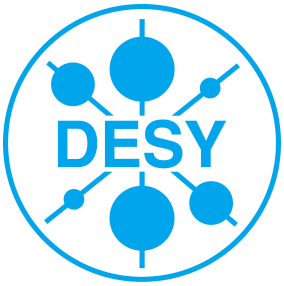

International Large Detector performance investigation

Oleksii Lubynets, Kiev National University, Ukraine

Supervisor: Shaojun Lu, DESY, Germany

September 6, 2017

Abstract

The International Large Detector (ILD) is a concept for a detector at the International Linear Collider, ILC. The ILC has an ambitious physics program, which will extend and complement that of the Large Hadron Collider. A hallmark of physics at the ILC is precision.
In this work one ILD optimisation model (ILD_s4_v02) performance has been studied. We evaluate the impact parameter and momentum resolution, tracking efficiency and linearity of energy reconstruction with both single particles and $t\bar{t}$-events.

Contents

1 Introduction

The International Large Detector (ILD) is a concept for a detector at the International Linear Collider, ILC. The ILC will be a particle accelerator to collide electrons against positrons at energies from 250 GeV to 1 TeV. The ILC has an ambitious physics program, which will extend and complement that of the Large Hadron Collider. A hallmark of physics at the ILC is precision. To take full advantage of the physics potential of ILC places great demands on the detector performance. The ILD design is driven by this requirements.
The ILC is designed to investigate in detail the mechanism of the electroweak symmetry breaking, and to search for and study new physics at energy scales up to 1 TeV. In addition, the collider will provide a wealth of information on Standard Model physics, for example top physics, heavy flavour physics, and physics of the Z and W bosons. The requirements for a detector are, therefore, that multi-jet final states, typical for many physics channels, can be reconstructed with high accuracy. The jet energy resolution should be sufficiently good that the hadronic decays of the W and Z can be separated. This translates into a jet energy resolution of $\frac{\sigma_E}{E} \sim 3-4\%$. This requirement is one of the most challenging for ILD and has a large impact on the design of the calorimeters. It also impacts the way the tracking system is optimised. Nevertheless, the reconstruction of events with high precision benefits the ILD physics programme in several ways. A more precise detector will result in smaller systematic errors for many measurements, and thus will extend the ultimate physics reach of the ILC. In addition, a more precise detector implies that the luminosity delivered by the collider is used more efficiently. [1]

2 The ILD technical design overview

The ILD detector is strongly influenced by two basic assumptions about experimentation at a linear collider: particle flow as a way to reconstruct the overall event properties, and high resolution vertexing. Particle flow calorimetry requires a reliable tracking system which enables charge particle momenta to be reconstructed with high precision. ILD is built around a calorimeter system with very good granularity both in the transverse and in the longitudinal direction, and a combination of silicon and gaseous tracking systems. Vertexing, the other great challenge, is addressed to a high precision pixelated detector very close to the interaction point.
Figure 1 illustrates the ILD_s4_v02 detector and "true" (Monte-Carlo) particles.

2.1 Vertex detector

The Vertex Detector (VTX) is the key to achieving very high performance flavour tagging by reconstructing displaced vertices. It also plays an important role in the track reconstruction, especially for low momentum particles which dont reach the main tracker or barely penetrate its sensitive volume because of the strong magnetic field of the experiment, or due to their shallow production angle. The flavour tagging performance

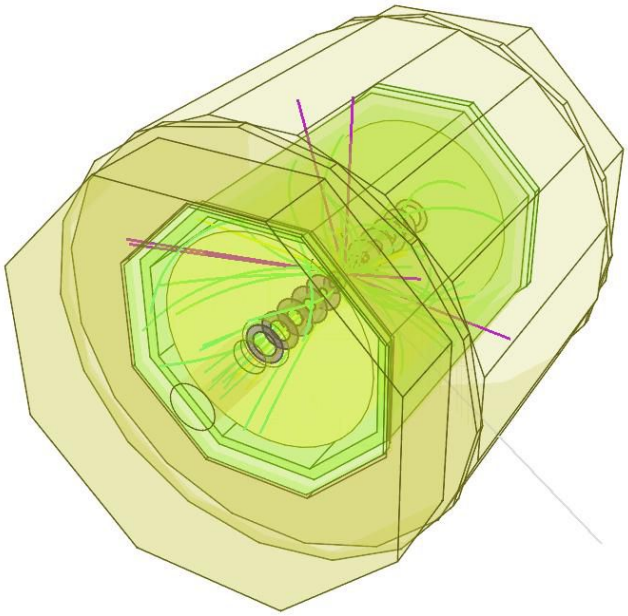

Figure 1: *ILD_s4_v02 and mc-particles. The yoke detector geometry is not shown.*

needed for physics implies that the first measured point on a track should be as close as possible to the IP.
The VTX is made of 6 cylindrical layers, all equipped with $\lesssim 50\ \mu m$ thin pixel sensors providing a single point resolution of 2.8 μm all over the sensitive VTX area. The innermost layer has a radius 16 mm, a value for which the beam-related background rate is expected to still be acceptable. As a consequence, the innermost layer intercepts all particles produced with a polar angle (θ) such that $|cos(\theta)| \lesssim 0.97$.

2.2 Silicon tracking

The tracking system of the ILD is optimised to deliver outstanding resolution together with excellent efficiency and redundancy. The choice of ILD is a combination of gaseous tracking, giving a large number of hits, and the redundancy this gives, with a sophisticated system of silicon based tracking disks and barrels. Together the system achieves excellent resolution, and covers the solid angle down to the very forward region.
The Silicon tracker is made of two sets of detectors:

- The first set is located in the central barrel and is made of the SIT (Silicon Internal Tracker), and the SET (Silicon External Tracker). The SIT is positioned in the radial gap between the vertex detector and the Time Projection Chamber (TPC) (see Section 2.3). The role of the SIT is to improve the linking efficiency between the vertex detector and the TPC; it improves the momentum resolution and the

reconstruction of low p_T charged particles and improves the reconstruction of long lived stable particles. The SET is located in the barrel part between the TPC and the central barrel electromagnetic calorimeter (ECAL). The SIT and SET provide time-stamping information for separation between the bunches and thus allowing the bunch-tagging of each event.

- The second set is located in the forward region and is represented by the FTD (Forward Tracking Detector) in the very forward region. The FTD is positioned in the innermost part of the tracking region, and covers the forward region down to about 0.15 radians. In total seven disks are foreseen in this region. The FTD ensures the full tracking hermeticity.

2.3 The time projection chamber

Two main aspects for tracking are:
1) The momentum of charged tracks must be measured with extremely high precision;
2) High resolution measurements of the jet-energy using the particle-flow technique require efficient reconstruction of individual particles within dense jets.

A TPC as the main tracker in a linear collider experiment provides high-precision measurements of three-dimensional r, ϕ, z space points. The TPC presents a low material budget as required for the best calorimeter performance.
Figure 2 illustrates reconstructed hits in VTX, Silicon Tracker and TPC.

2.4 The calorimeter system

Tagging of electroweak gauge bosons at the ILC, based on di-jet mass reconstruction, makes the reconstruction of multijet events a major goal for detectors at the ILC. The particle flow approach, which consists of individual particle reconstruction dictates many fundamental aspects of the calorimeter design, most notably the requirement for very fine transverse and longitudinal segmentation of the calorimeters.
The calorimeter system is divided in depth into an electromagnetic section, optimised for the measurement of photons and electrons, and a hadronic section dealing with the bulk of hadronic showers. The two parts are installed within the coil to minimise the inactive material in front of the calorimeters. The calorimeter is divided into a cylindrical barrel and two end-caps.
The electromagnetic calorimeter consists of tungsten absorber plates interleaved with layers of silicon detectors with very fine segmentation of the readout. The hadronic calorimeter is planned as a sampling calorimeter with steel absorber plates and fine grained readout. It consists of scintillator cells with fine granularity and multi-bit (analogue) readout.
Figure 3 illustrates showers, reconstructed in the calorimeter part of detector.

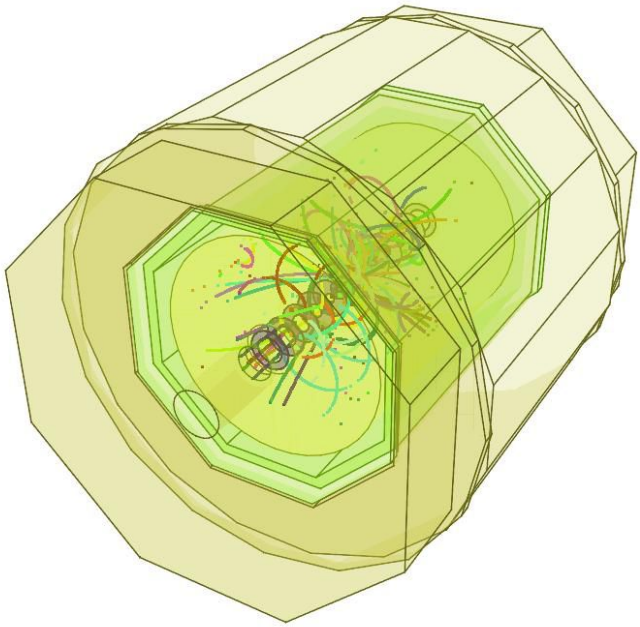

Figure 2: *ILD_s4_v02 and reconstructed data in tracking part (the yoke detector geometry is not shown).*

2.5 Other elements of the detector system

- Special calorimeters are foreseen in the very forward region of the ILD near the interaction point - LumiCal for the precise measurement of the luminosity and BeamCal for the fast estimate of the luminosity.

- The basic layout of the ILD detector has always followed the strategy of tracking in a magnetic field. The ILD_s4_v02 design therefore asks for a 4 T field in a large volume, with a high field homogeneity within the TPC volume and with a reduced fringe field outside the detector. The magnet consists of the superconducting solenoid, including the correction coils, and of the iron yoke, one barrel yoke in three pieces and two end-cap yokes, also in two pieces each. The yoke also includes detectors for tail catching and muon detection.

- Muon detector. The identification of leptons is an important part of the physics programme at the ILC. For muons above a few GeV, the instrumented iron return yoke is used as a high efficiency muon identifier. The clean environment of an electron-positron Linear Collider allows for a muon system design that is much simpler compared to the ones that have been developed for the hadron colliders. There is no need to trigger on muon tracks; instead the clean nature of the events at the ILC allows the linking of track candidates from the inner detectors with tracks in the muon system. The muon system in ILD will cover a large area of several

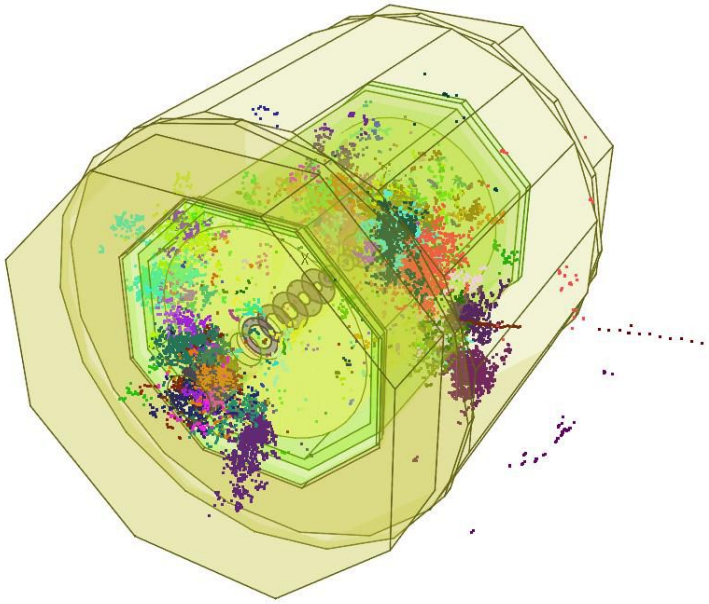

Figure 3: *ILD_s4_v02 and reconstructed showers in calorimeters (the yoke detector geometry is not shown).*

thousand square meters. The system will serve primarily as a muon identifier, but will also play an important role as a tail catcher to compensate for leakage from the calorimeter system. [1]

3 Detector characteristics investigation

Our aim is to evaluate the momentum and impact parameter resolution, precision of track parameters determination, tracking efficiency. We use the *iLCSoft* software framework with the *Marlin* [2] application framework. We simulate the process of particle production in electron-positron collisions. Then we simulate particles propagation through the detector system based on Geant4 [3]. After that we perform reconstruction of tracks, vertices and particles.

3.1 Track parameters pull distribution

Each track is a part of a helix (the trajectory of the particle is curved due to the magnetic field, and moving along the z-axis is not perturbed). The track is characterized with the following 5 parameters:

- d_0, impact parameter in the xy-plane.

- ϕ_0, azimuthal angle of the momentum of the particle (track tangent) at the point of the closest approach (PCA) to the reference point (usually (0; 0; 0)) in the xy-plane.
- Ω, the curvature of the track. $|\Omega| = \frac{1}{R}$.
- z_0, the z-coordinate of the PCA.
- $\tan\lambda$, the slope $\frac{dz}{ds}$, where s is the arc length in the xy-plane.

The sign of d_0, Ω and $\tan\lambda$ is defined with the direction of particle moving along the track. [4]

To monitor the reconstruction performance we use single muons with different momentum at different directions. To estimate, how much the error of track parameter reconstruction is, we investigate the pull distribution: $pull(A) = \frac{A_{reco} - A_{sim}}{\sigma_A}$, where
A stands for any of track parameter (d_0, ϕ_0, Ω, z_0, and $\tan\lambda$);
index *reco* means the reconstructed value of A;
index *sim* means the "true" value of A from the simulation;
σ is the standard error of the reconstructed value.

The final fit of pull distribution is shown in Fig. 4 and 5. We observe the bias from expected values (0 for mean, 1 for sigma), and the bias is larger for small P_T and small θ (corresponds to the forward region).

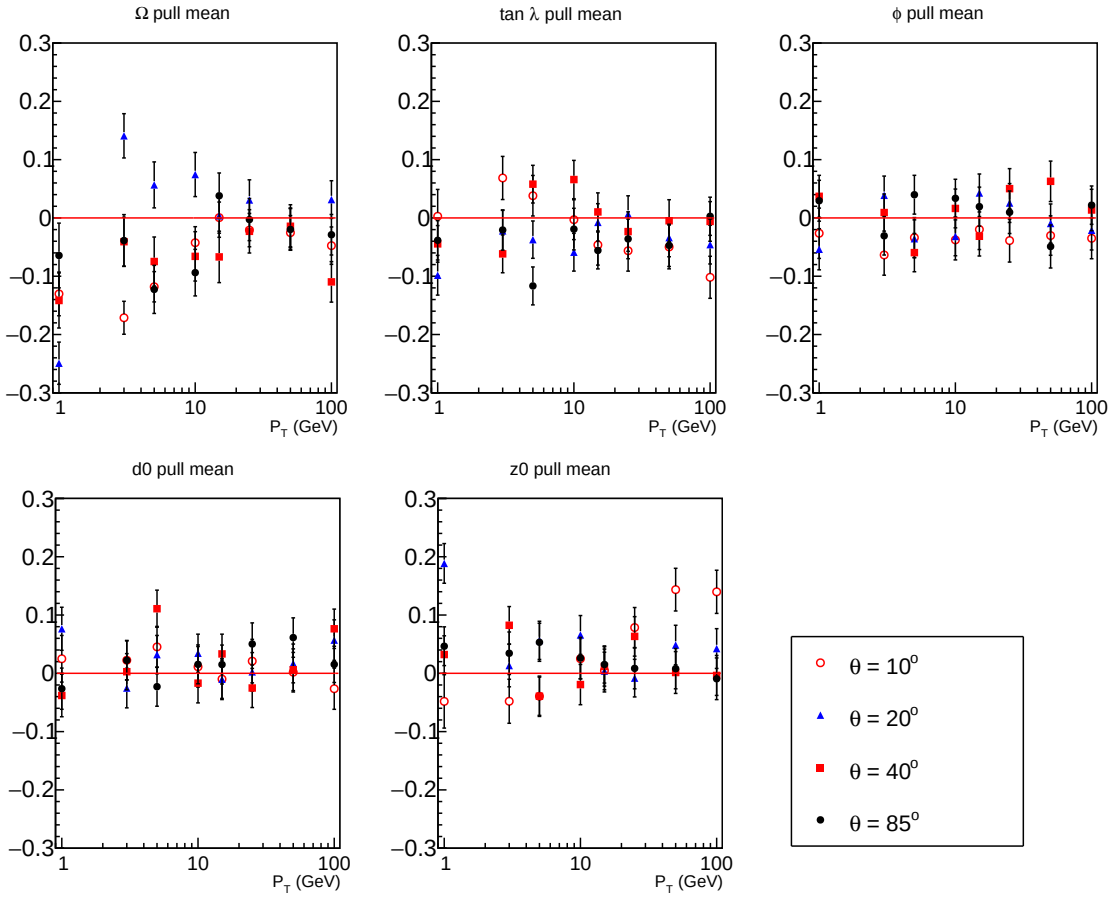

Figure 4: *Pull mean values.*

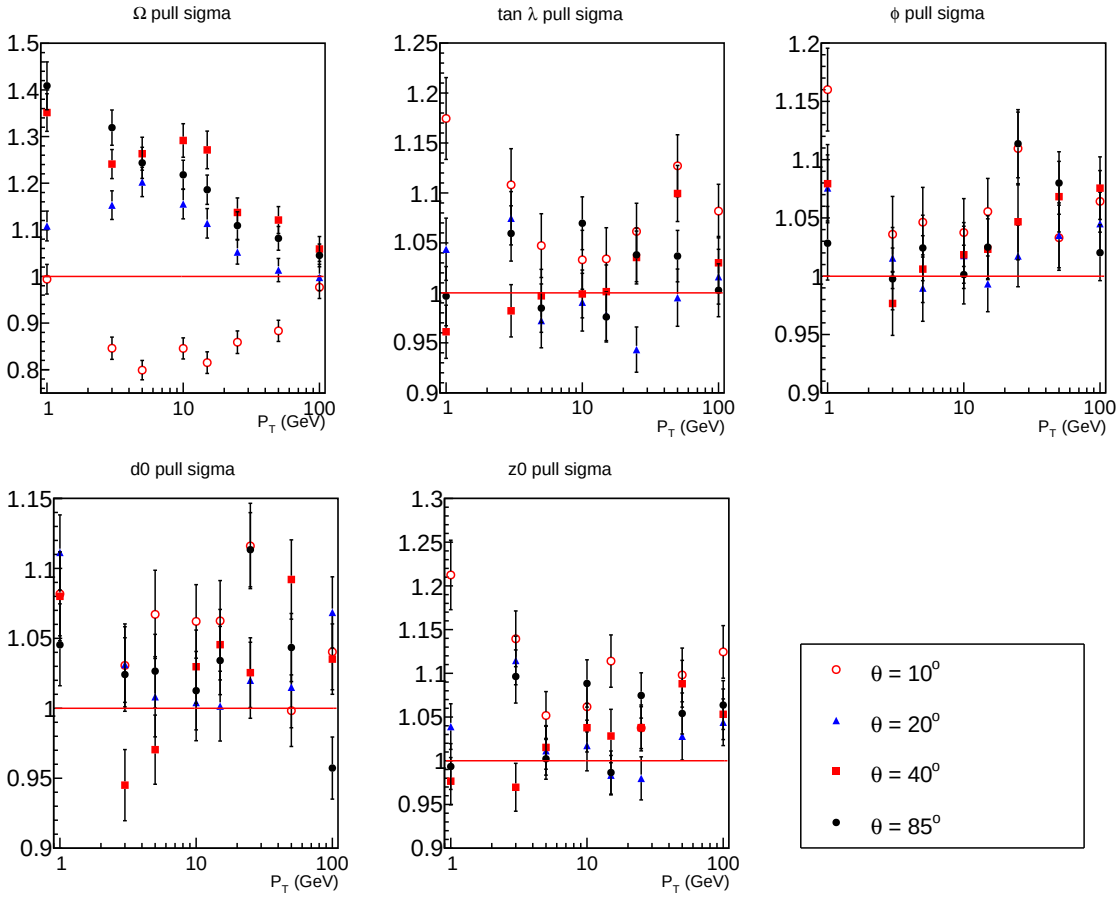

Figure 5: *Pull sigma values.*

3.2 Resolution of the tracking part of detector

We simulate propagation of muons through the detector system with different values of transverse momentum and polar angle (1000 muons for each pair "Momentum - Polar angle"). Each muon is characterised with certain values of impact parameter (distance from the point of muon production to the z-axis) and transverse momentum. And for each muon the mentioned values are reconstructed. If we had a perfect reconstruction, the simulated and reconstructed values would be equal, but in general case they are not.

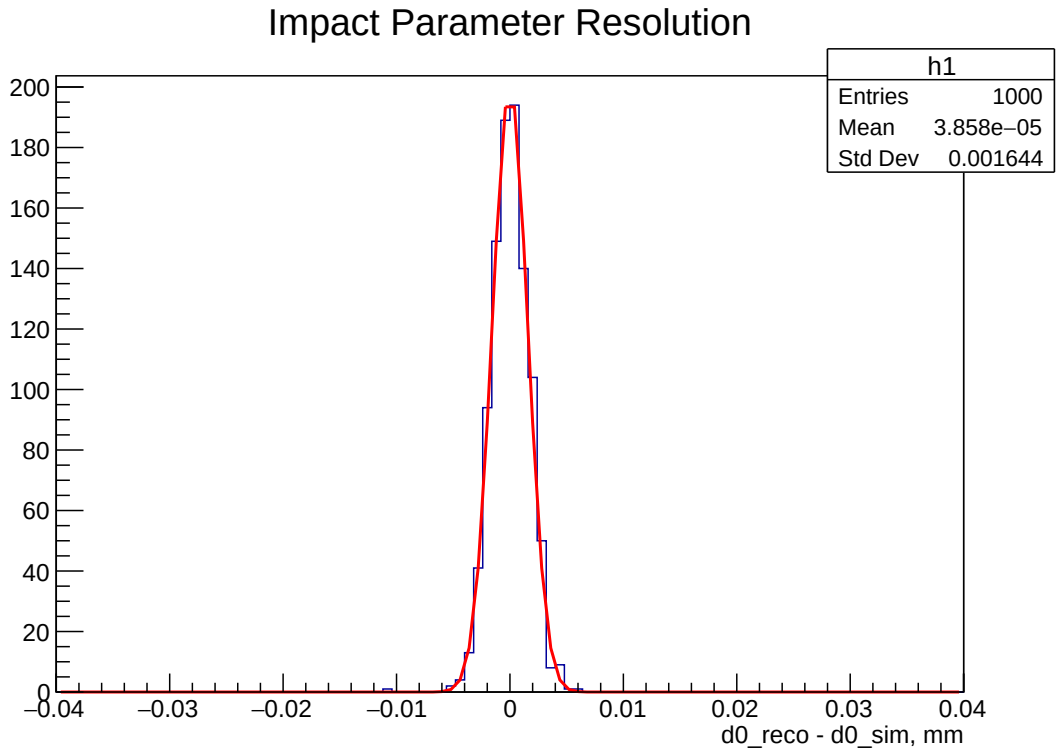

Figure 6: *Distribution of reconstructed impact parameter for 100-GeV muons with 85° polar angle.*

So, we build the distribution of difference between reconstructed and simulated values of impact parameter (see Fig.6). (For the transverse momentum we divide the difference by square of the simulated momentum). According to the central limit theorem this distribution is Gaussian. The standard deviation of this distribution σ defines the resolution. Figures 7 and 8 illustrate the IP and P_T resolution for different values of momentum and polar angle.

We observe the following regularity: IP and P_T resolution decreases when transverse momentum increases and polar angle increases. This can be explained in the following way: when the P_T is small, the track curvature is large (radius is small), and the muon does not propagate through the whole tracking system. And small values of polar angle

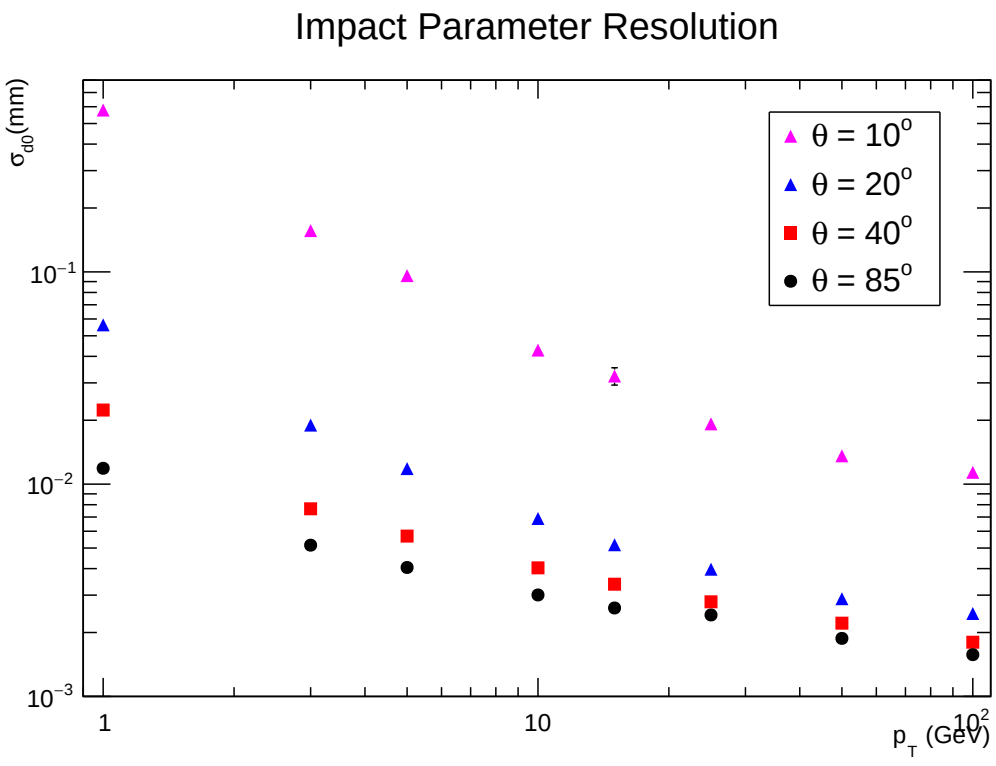

Figure 7: *Impact parameter resolution.*

mean that muon does not reach the barrel, instead of this it faces the forward detector. All this leads to increasing of the resolution.

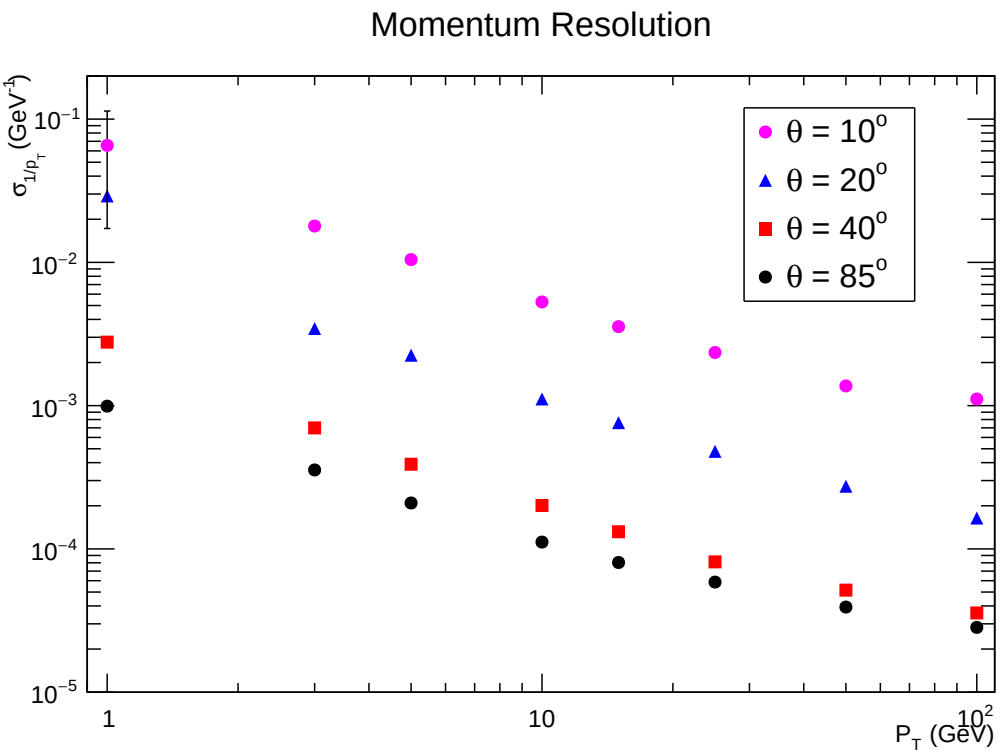

Figure 8: *Transverse momentum resolution.*

3.3 Tracking efficiency

Not all of charged particles are reconstructed. Here is the definition of the tracking efficiency:
$\varepsilon = \frac{N_{matched}}{N_{findable}}$, where
$N_{findable}$ is the number of tracks, which *can* be reconstructed in principle;
$N_{matched}$ is the number of reconstructed tracks matched with simulated tracks.
Figure 9 illustrates the tracking efficiency depending on values of transverse momentum and $\cos(\theta)$.

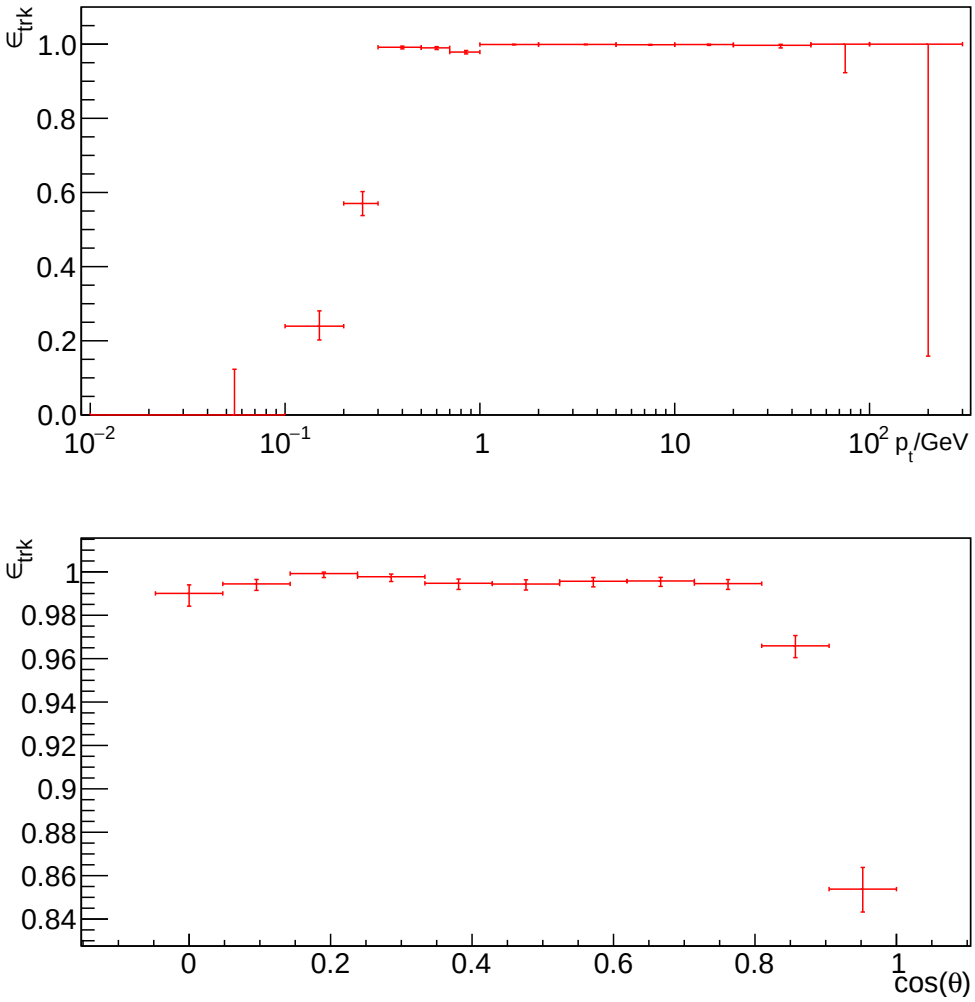

Figure 9: *Tracking efficiency.*

We observe, that the tracking efficiency increases with transverse momentum and reaches almost 100%. In opposite, the efficiency is small, when the transverse momentum is small. It can be explained in the following way: particles with small transverse momen-

tum do not propagate through the whole tracking system. The same can be said about particles with small polar angle.
Then we apply cuts to the transverse momentum and absolute value of momentum: we consider only particles with $P > 1\ GeV$ and $P_T > 0.5\ GeV$ (see Fig.10). We observe a significant increasing of tracking efficiency.

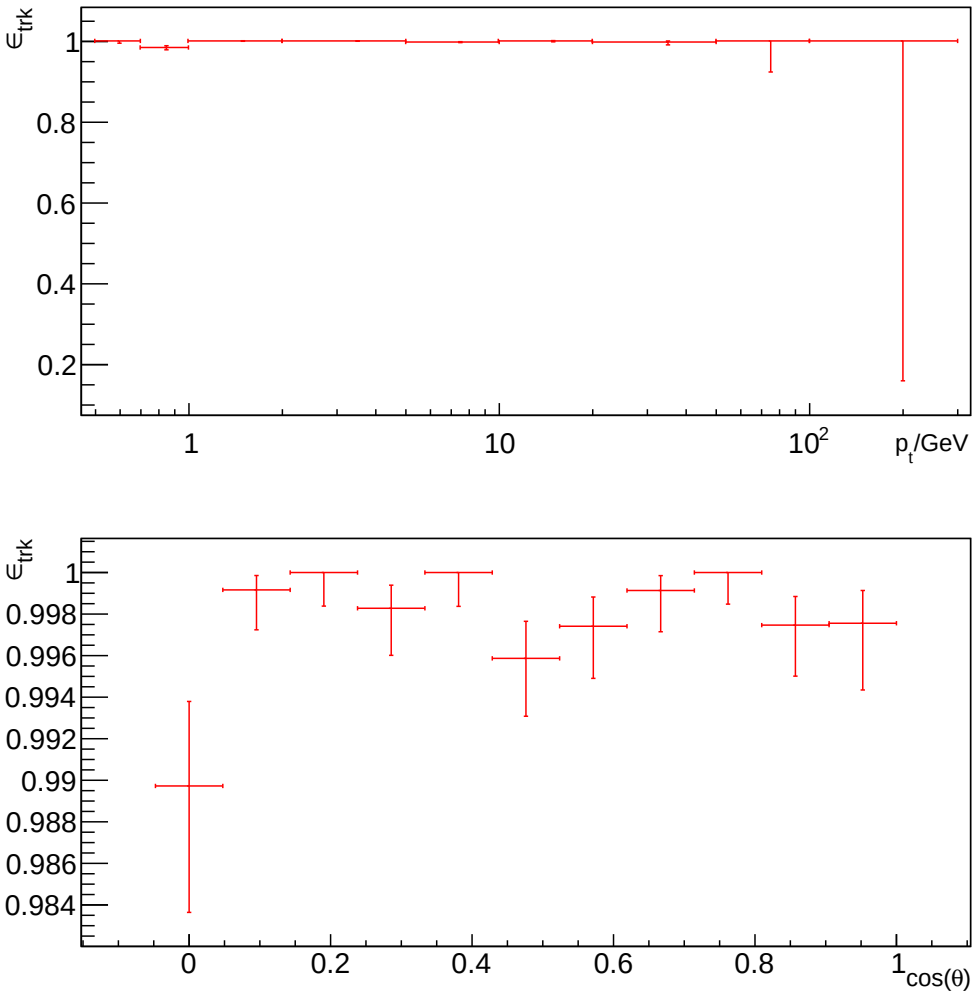

Figure 10: *Tracking efficiency with* $P > 1\ GeV$ *and* $P_T > 0.5\ GeV$ *cuts.*

3.4 Linearity of single particle energy reconstruction

The momenta of charged particles are measured in the tracking detectors, while the energy measurements for photons and neutral hadrons are obtained from the calorimeters. We provide energy reconstruction (1, 2, 5, 10, 20, 50, 100 GeV) for 9 kinds of particles (e^-, μ^-, γ, π^0, K_L^0, π^+, K_S^0, K^+, p^+). Then we build the distribution of reconstructed energy (see Figures 11 and 12), fit it with Gaussian, and the mean value of this distribution we assume to be the reconstructed energy.

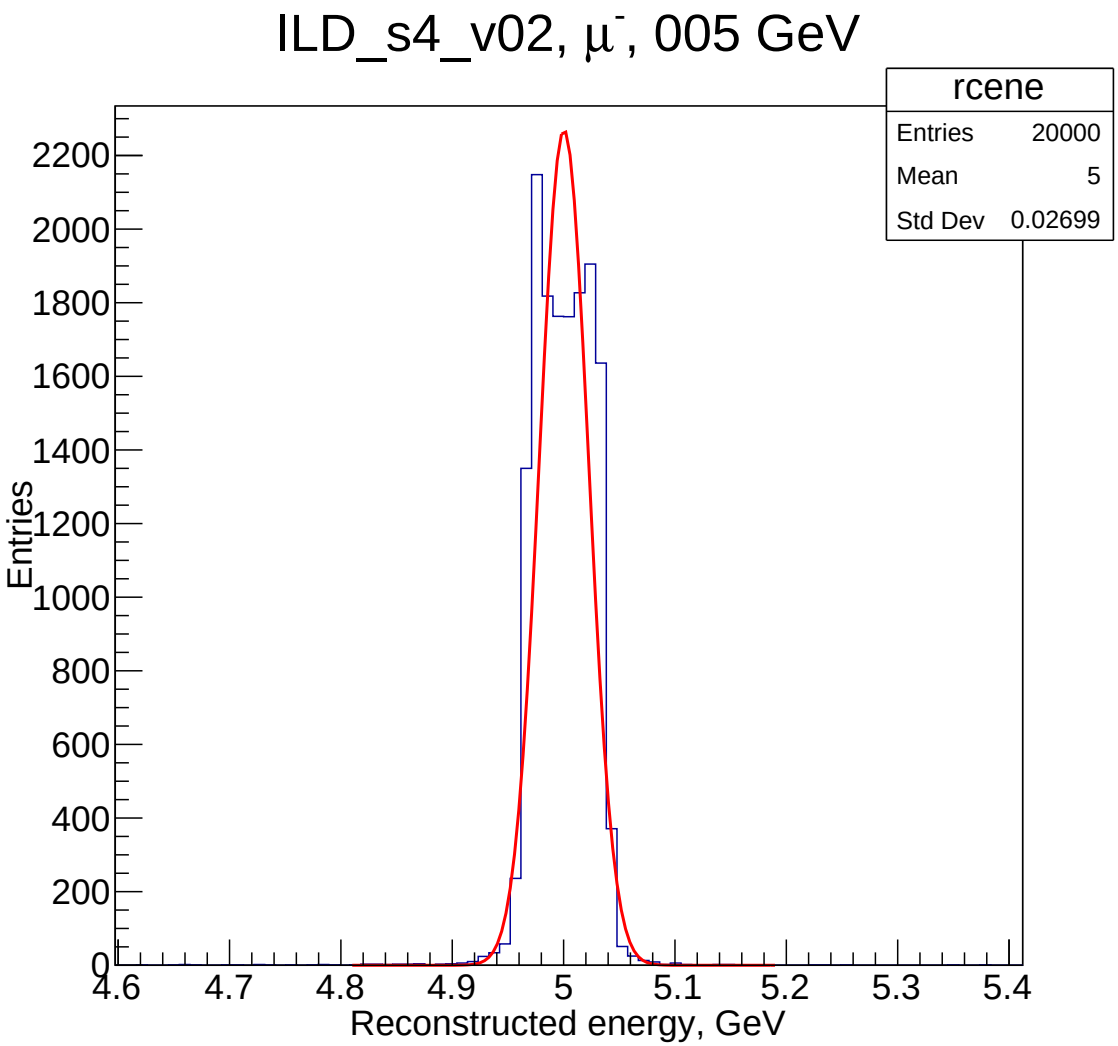

Figure 11: *Reconstructed energy distribution for 5 GeV muon.*

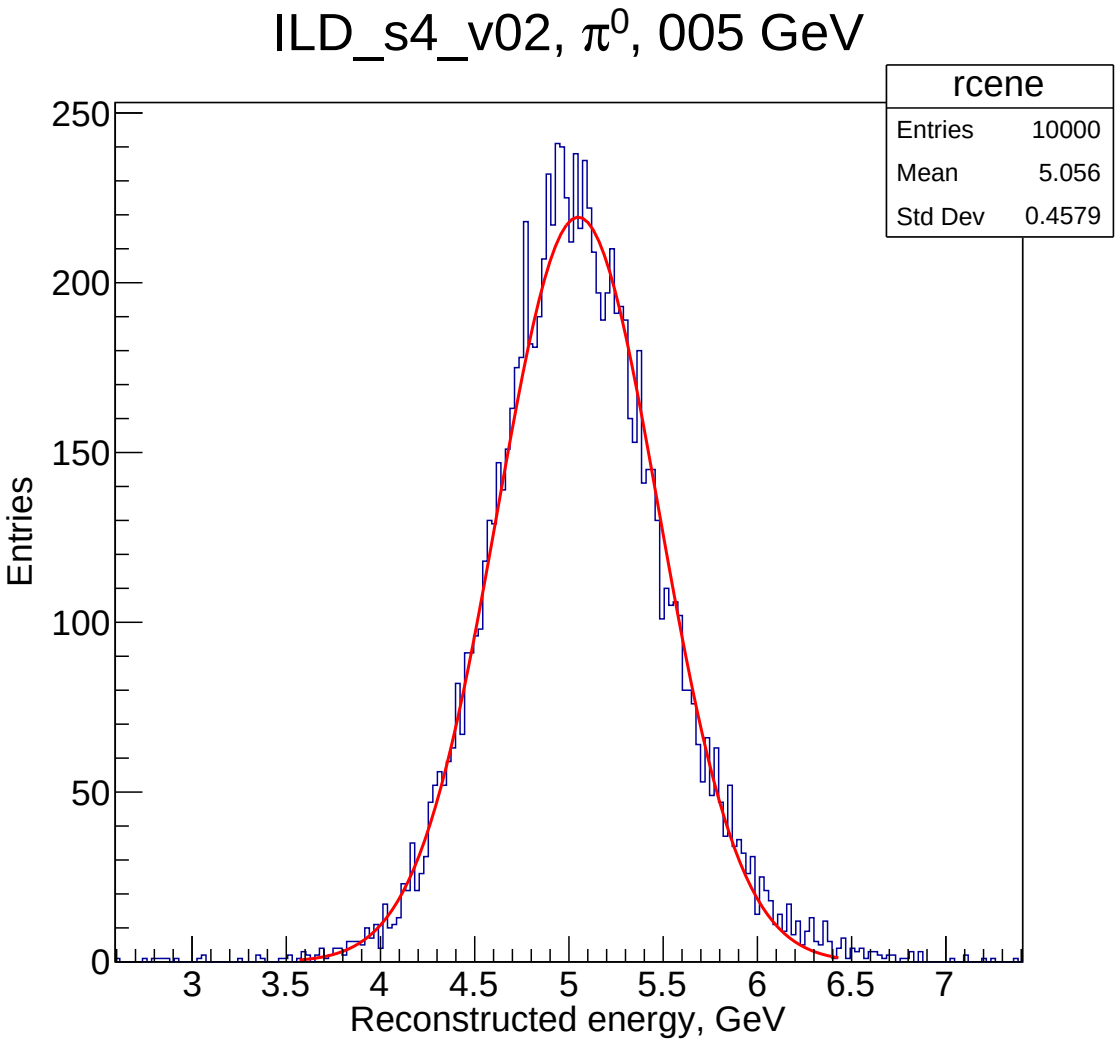

Figure 12: *Reconstructed energy distribution for 5 GeV pion.*

Figures 13 - 21 illustrate the reconstructed energy versus its "true" value.

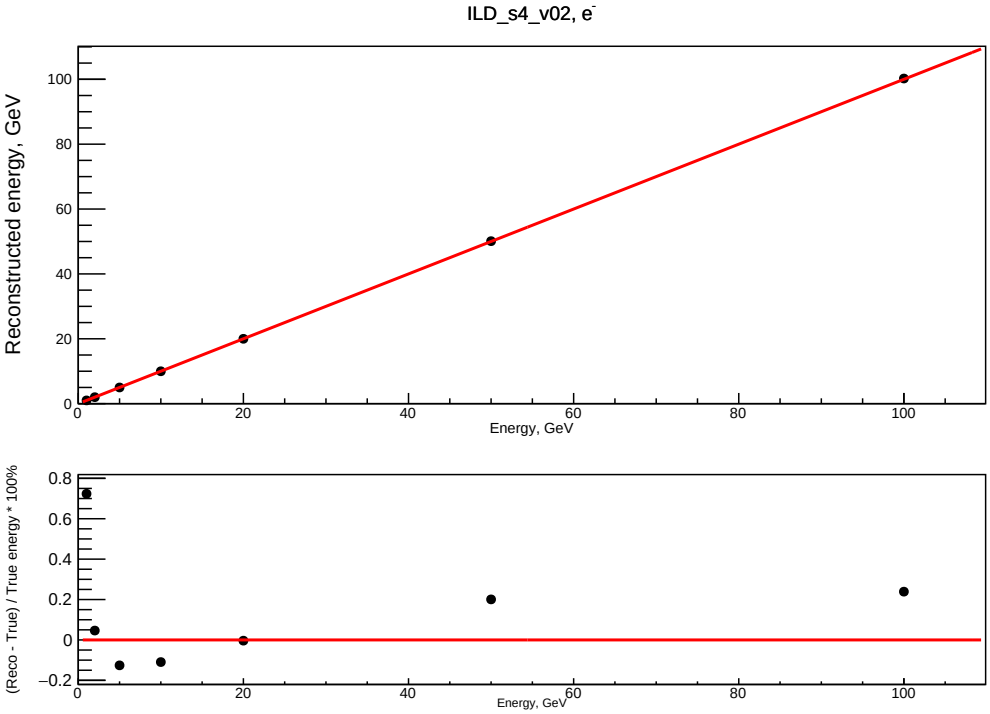

Figure 13: *Reco vs Mc energy for* e^-.

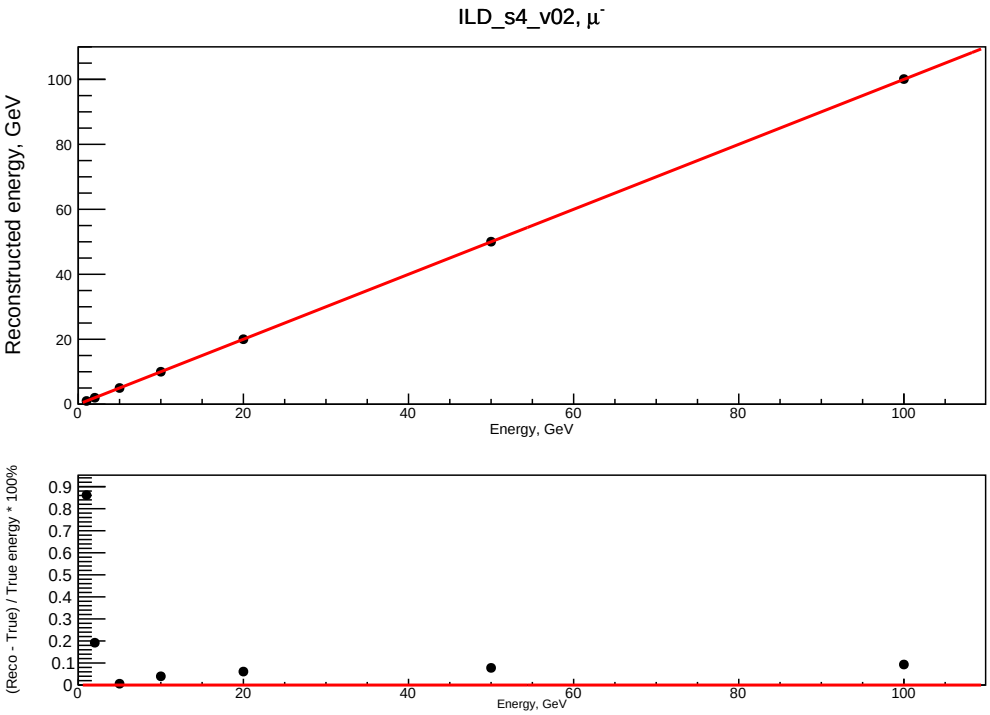

Figure 14: *Reco vs Mc energy for* μ^-.

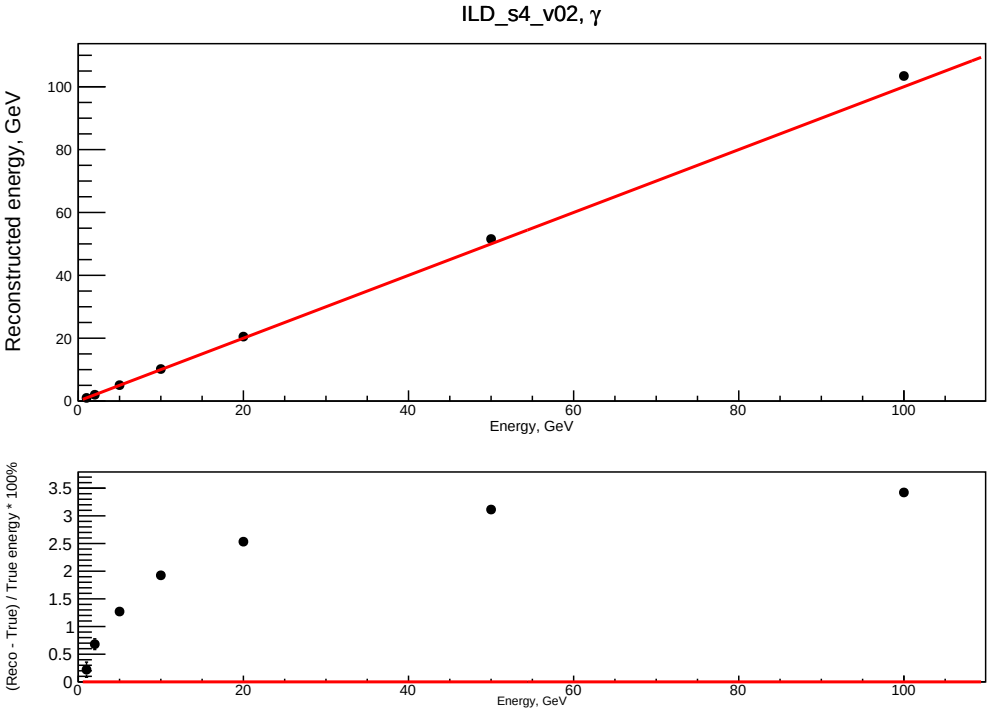

Figure 15: *Reco vs Mc energy for* γ.

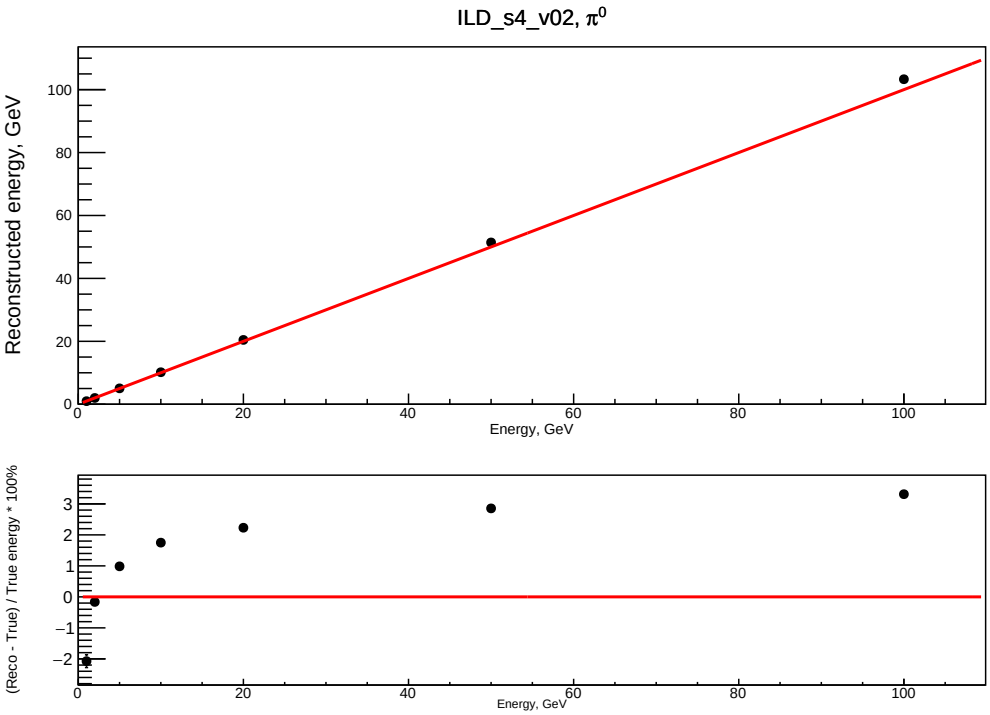

Figure 16: *Reco vs Mc energy for* π^0.

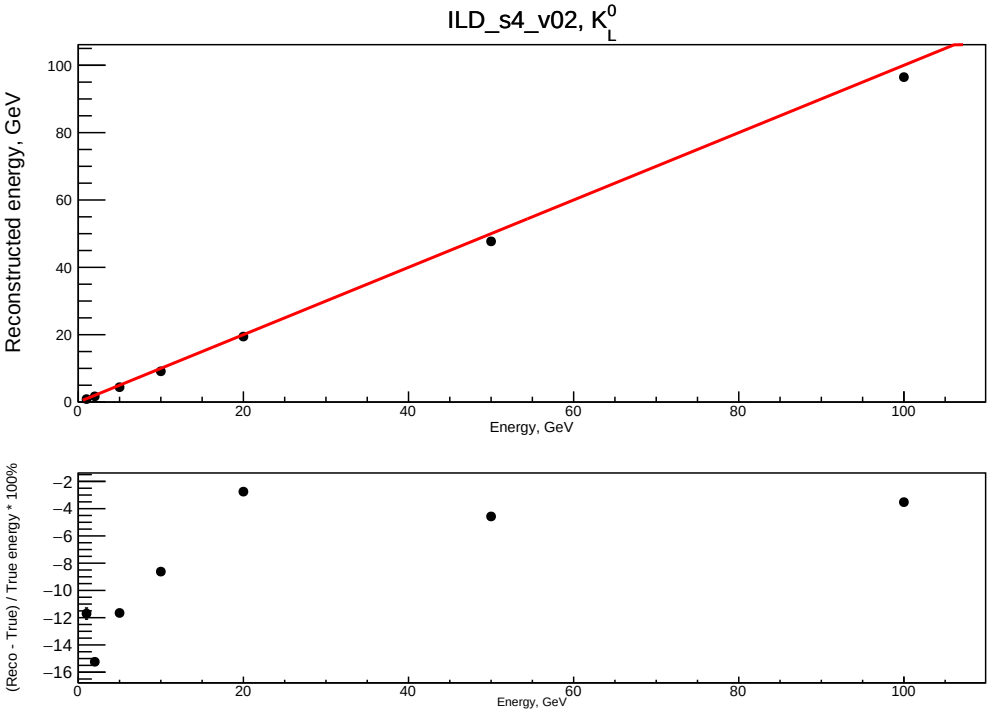

Figure 17: *Reco vs Mc energy for* K_L^0.

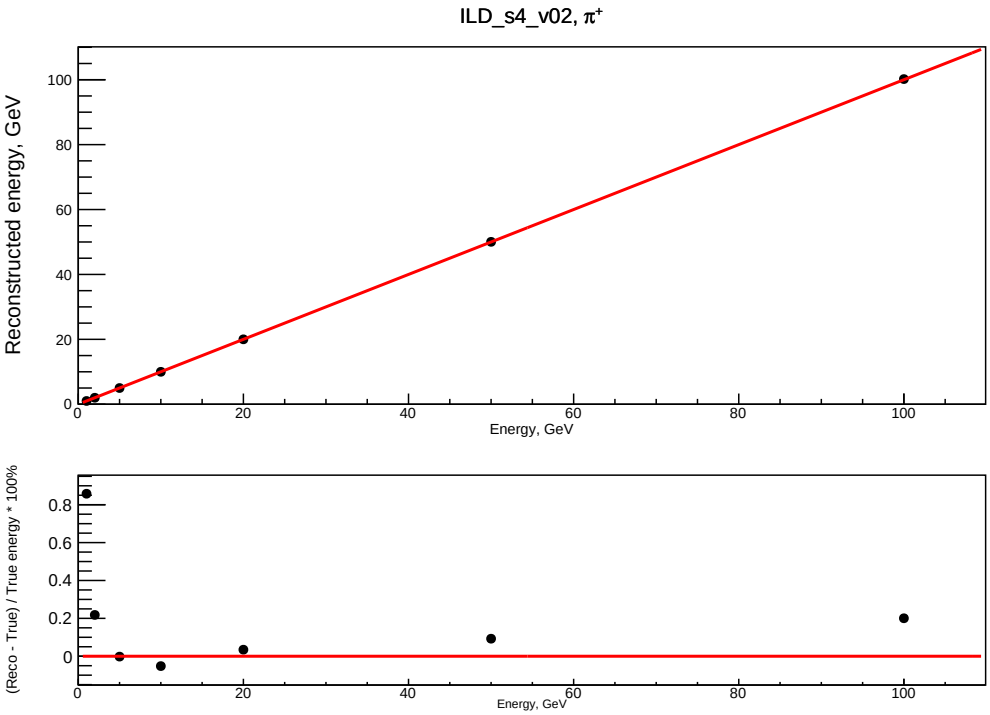

Figure 18: *Reco vs Mc energy for* π^+.

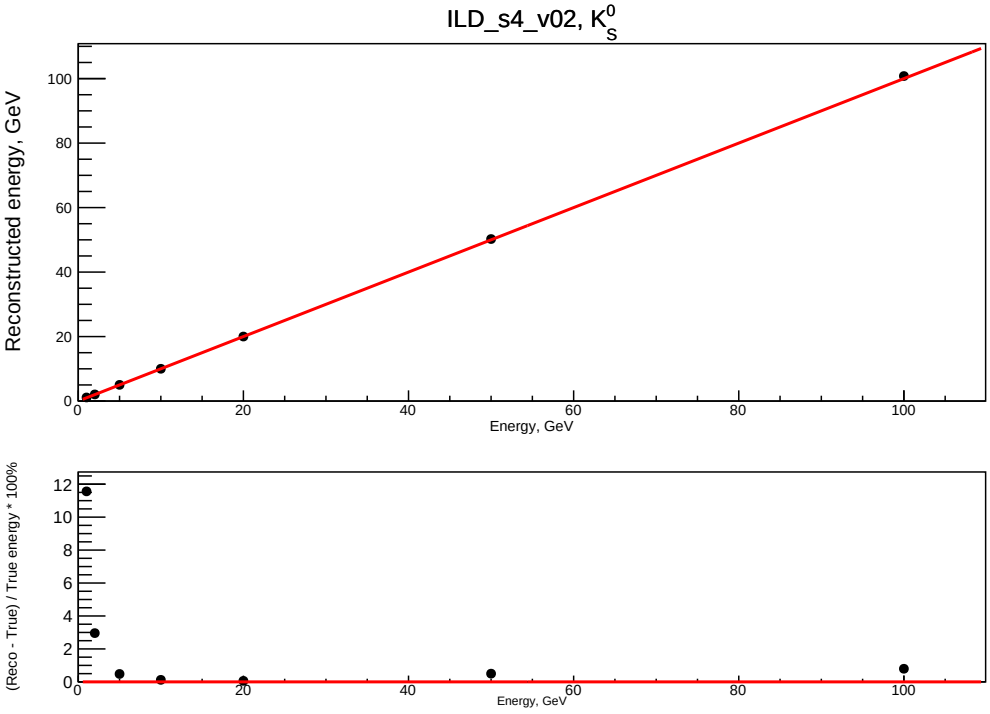

Figure 19: *Reco vs Mc energy for* K_S^0.

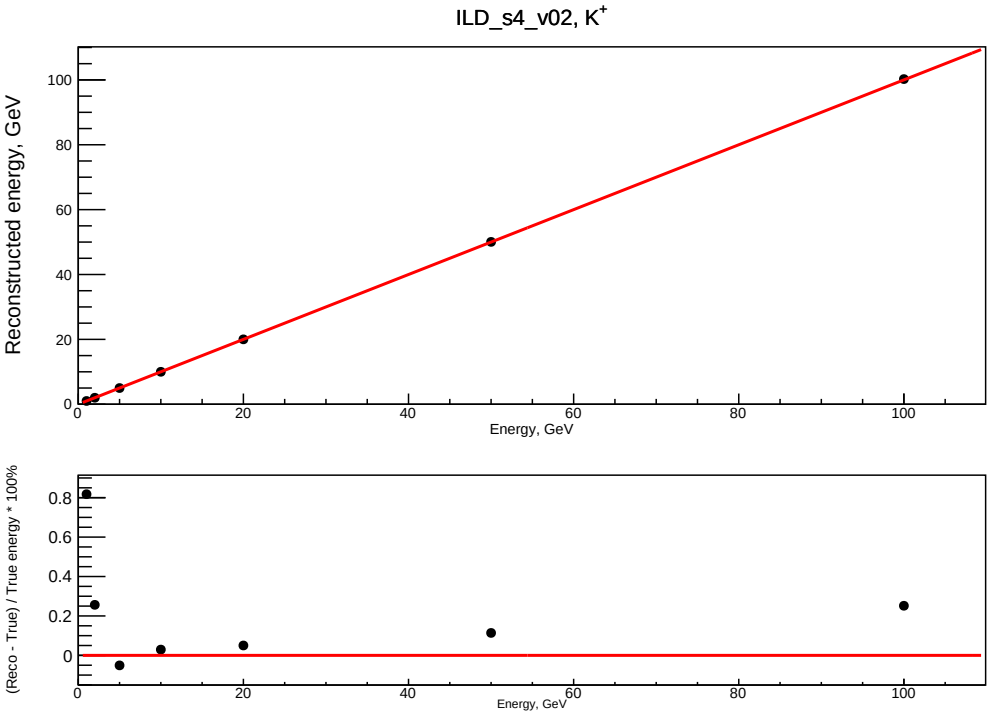

Figure 20: *Reco vs Mc energy for* K^+.

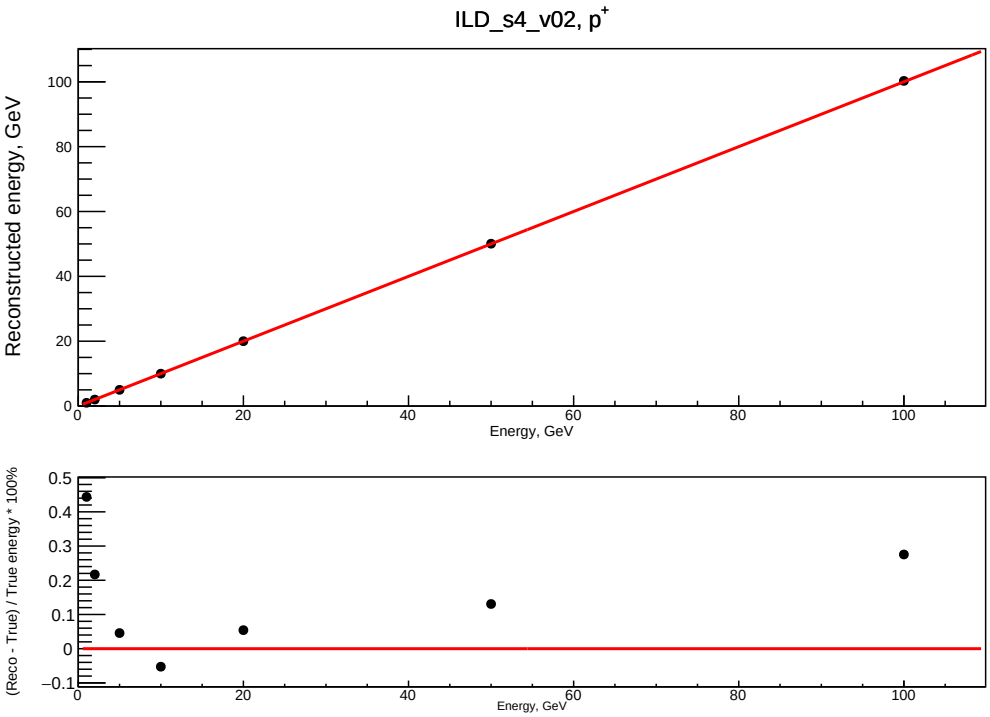

Figure 21: *Reco vs Mc energy for* p^+.

The following features of reconstructed energy distribution worth be noted:

- Reconstructed energy distribution of neutral particles (except of K_S^0) is broad (see Fig.12).
- In contrast, reconstructed energy distribution of charged particles (and K_S^0) is "sharp", narrow (see Fig.11).
- Difference between reconstructed and "true" energy is smaller for charged particles and larger for neutral particles (see Figures 13 - 21).
- Difference between reconstructed and "true" energy has different signs for different particles: for majority of particles it is positive (energy is overestimated); for K_L^0 it is negative (we underestimate the reconstructed energy).

The first three features can be explained with fact, that charged particles may be detected with both tracking and calorimeter parts of detector, and neutral particles - only via calorimeter. K_S^0 behaviour is similar to charged particles because of two facts: (a) K_S^0 decays into $\pi^+\pi^-$ with branching ratio 69.2%[5], and (b) K_S^0 lifetime equals $c\tau = 2.7\ cm$, so it decays inside the tracking part of detector. Other neutral particles (π^0, γ) do not decay into charged or have much larger lifetime (K_L^0, $c\tau = 15\ m$) and propagate through the tracking part without decay.
The last feature can be explained with fact, that different particles are detected and measured with different parts of detector (γ - with ECal, e^- - with VTX, Silicon Tracker and ECal, K_L^0 - with HCal etc). Each detector part is calibrated separately. So, different types of particles help us to investigate performance of different parts of detector.

4 Conclusions

In this project the characteristics of ILD_s4_v02-version ILC detector have been studied with both single particles and $t\bar{t}$ events. In the track parameters pull distribution there is bias for lower P_T and $\theta = 10^\circ$ (corresponds to forward region).
The momentum and impact parameter resolution is better for large P_T and $\theta = 85^\circ$ (barrel region), as we expected.
The tracking efficiency at 90° is a little bit lower, than for other directions. This fact need to be understood.
Linearity of single charged particles energy reconstruction is better than of neutral particles. For the neutral particles the ECal, HCal and pandora (algorithm) have not yet calibrated perfectly. We expect the linearity will be improved after calibration.

5 Acknowledgements

I would like to thank my supervisor Dr. Shaojun Lu for guidance of my work on the project and sharing experience, and Dr. Remi Ete for explaining the details of work (especially concerning the calorimeter part of detector). Also I am thankful to all the lecturers and organizers of DESY Summer Student Programme for the opportunity to take a part in such an interesting activity.

References

[1] The International Large Detector. Letter of Intent. *ILD Concept Group*

[2] Marlin and LCCD: Software tools for the ILC. Nucl.Instrum.Meth., A559:177-180, 2006. *F. Gaede*

[3] GEANT - Detector Description and Simulation Tool, CERN Program Library Long Writeup W5013 *R. Brun*

[4] Track Parameters in LCIO, LC-DET-2006-004. *Thomas Kraemer, DESY-FLC*

[5] Particle Data Group, pdg.lbl.gov.